Hindawi
Advances in Polymer Technology
Volume 2023, Article ID 7484634, 11 pages
https://doi.org/10.1155/2023/7484634

Research Article

Preparation and Properties of Boron Nitride or Aluminum Nitride Reinforced Glass Fiber/Modified Polyphenylene Sulfide Composites

Jingxian Zhao, Shijie Cai, Xiaolu Chen, Haohao Ren, and Yonggang Yan

College of Physics, Sichuan University, Chengdu, China

Correspondence should be addressed to Yonggang Yan; yan_yonggang@vip.163.com

Received 24 November 2022; Revised 21 March 2023; Accepted 22 March 2023; Published 11 April 2023

Academic Editor: Puyou Jia

In this work, polyphenylene sulfide (PPS) containing carboxyl group was synthesized and used to prepare PPS-2COOH/LGF/AlN and composites with high-temperature resistance, corrosion resistance, low dielectric constant, and low dielectric loss were prepared with boron nitride/aluminum nitride (BN/AlN) and glass fiber (LGF). The results showed that the introduction of carboxyl groups did not affect the structure and thermal properties of PPS. The composites exhibited good mechanical properties with a tensile strength of 65 MPa~97 MPa and flexural strength of 112 MPa~154 MPa. The TGA results showed that the composites had good thermal stability, and the $T_{5\%}$ of PPS-2COOH/LGF/AlN (20) and PPS-2COOH/LGF/BN (20) reached up to 511.6°C and 506.3°C, respectively. They were insoluble in some organic solvents, such as NMP and DMF at room temperature, and they exhibited excellent chemical resistance. The dielectric performance results showed that with the increase of frequency, the dielectric constant and dielectric loss gradually decreased, the dielectric constant of PPS-2COOH/LGF/BN (15) was 3.9, and the dielectric loss of PPS-2COOH/LGF/BN (15) was 0.01. From the above results, it can be concluded that the composite materials PPS-2COOH/LGF/AlN and PPS-2COOH/LGF/BN have potential application prospects in the field of 5G high thermal conductivity materials.

1. Introduction

With the introduction of 5G communication technology, higher standards for materials have been established [1]. Dielectric polymer composites are carefully explored and widely employed as a key substrate for electronic packaging and energy storage [2, 3], and they must meet the substrate materials with the least amount of reduction in high-frequency (millimeter wave) signal transmission speed, i.e., a small dielectric constant, a small dielectric loss, a high glass transition temperature, a small coefficient of thermal expansion, and a high thermal conductivity [4, 5].

The molecular structure of polyphenylene sulfide (PPS) is alternately structured by benzene rings and sulfur atoms, and the configuration is tidy, making it easier to produce a crystalline structure with excellent thermal stability [6, 7]. The benzene ring makes it high in mechanical properties, heat resistance, and flame retardant properties, which can effectively replace metal parts in many applications, reduce weight, and reduce costs [8]. However, due to the low thermal conductivity and poor heat dissipation performance of polyphenylene sulfide itself, its application had been limited in some areas.

A simple and effective strategy for improving the thermal conductivity of polymers is the addition of high thermal conductivity fillers [9–12], such as silicon carbide [13, 14], alumina [15], boron nitride (BN) [16–19], aluminum nitride (AlN) [20, 21], carbon nanotubes [22, 23], graphene [24–26], entering the polymer matrix to form thermal conductivity paths and networks to enhance thermal conductivity [27]. Among these fillers, BN and AlN are widely used due to their excellent thermal conductivity and insulation. However, high thermal conductivity fillers enhance dielectric losses and reduce electrical breakdown strength. Moreover, if too much ceramic filler with high thermal conductivity is added, it will affect the mechanical properties

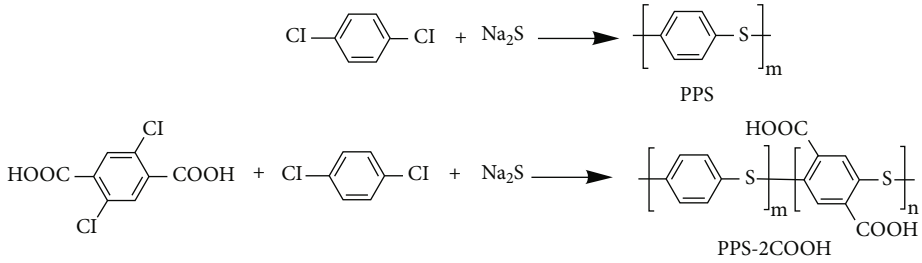

Scheme 1: Synthesis route of copolymer PPS-2COOH, m : n = 97.5 : 2.5.

Table 1: Composition of the PPS-2COOH/LGF/AlN and PPS-2COOH/LGF/BN composites in wt%.

Samples	PPS-2COOH (wt%)	BN (wt%)	AlN (wt%)	LGF (wt%)
PPS-2COOH/LGF/BN (15)	60	15		25
PPS-2COOH/LGF/BN (20)	55	20		25
PPS-2COOH/LGF/AlN (15)	60		15	25
PPS-2COOH/LGF/AlN (20)	55		20	25
PPS-2COOH/LGF	75			25

and density of PPS composites and also pose major challenges to the processing of composite materials. Guo et al. prepared aluminum nitride/polyphenylene sulfide (AlN/PPS) composites by melt blending method and found that excessive addition of AlN easily leads to aggregation and weakens mechanical properties [28]. To improve mechanical properties, glass fiber is widely used as a high-strength rigid reinforcing filler due to its low cost [29–33]. Among them, low dielectric glass fiber is widely used due to its low dielectric constant [34], TDL-GLASS (LGF) is a new type of low dielectric constant glass fiber, the frequency at 1 MHz frequency, its dielectric constant is about 4.3~4.6, the frequency is 10GHz, the dielectric constant can reach 4.2~4.3 [35, 36].

It can be seen from the above that PPS composites with high heat resistance, high thermal conductivity, and low dielectric constant are expected to be obtained by adding low dielectric glass fiber, BN, or AlN in PPS resin. However, the interface between PPS and filler is inert, which affects its mechanics and dielectric properties [37]. The methods to improve the interface generally include coupling agent treatment and interface compatibilizer modification [38, 39]. However, the coupling agent may volatilize at high temperatures due to its low boiling point. In general, the interface between the polymer and the filler can be improved by functionalizing the surface of PPS, such as carboxylation or amination. For example, PPS containing carboxyl groups can generally form hydrogen bonds with glass fibers, carbon fibers, etc., thereby improving the interaction between them and the matrix [40, 41]. The aminated PPS (PPS-NH_2) also could be used to improve the compatibility of CF with the PPS matrix [42]. Meanwhile, Yuan et al. synthesized carboxyl polyphenylene sulfide copolymers with low molecular weight and used them as sizing agents for CF/PPS composites [40, 43].

Therefore, in this work, PPS containing a double carboxyl group was synthesized and then used as the substrate to prepare composite materials containing BN and AlN. The properties such as thermal, mechanical, dielectric properties, and chemical corrosion resistance are also discussed in detail.

2. Experimental

2.1. Materials. Materials are 1,4-dichlorobenzene (99%, Shandong Pesticide), sodium sulfide ($Na_2S{\cdot}Xh_2O$ $Na_2S\%\approx45\%$) (Yuncheng Fengyuan Kechuang Chemical Co., Ltd), NaOH (AR, Chengdu, Chron Chemicals Co., Ltd.), HCl liquid (HCl%≈36%, Chengdu, Chron Chemicals Co., Ltd.), N-methyl-2-pyrrolidinone (NMP) (99%, Binzhou Yuneng Chemical Co., Ltd.), and ethyl alcohol (EtOH) (99.8%, Chengdu, Chron Chemicals Co., Ltd.). Boron nitride (BN, particle size: 3-7 microns) and 2,5-dichloroterephthalic acid (98%), purchased from Zhengzhou Alpha Chemical Co., Ltd. LGF was provided by Taishan Fiberglass Inc. Aluminum nitride (AlN, particle size: 2-9 microns) was prepared by the Ceramics Research Group of Physics College, Sichuan University.

2.2. Copolymer Synthesis. According to Scheme 1, the modified PPS resin was synthesized by a nucleophilic substitution reaction with 1,4-dichlorobenzene, 2,5-dichloroterephthalic acid, and sodium sulfide in NMP at high pressure. First of all, 173.35 g of sodium sulfide (1 mol, $Na_2S{\cdot}xH_2O$ $Na_2S\%\approx45\%$), 4.00 g NaOH (0.05 mol), an appropriate amount of catalyst [44], and 500 mL of NMP were added into the high-pressure reactor. Stirred, heated with nitrogen, and then gradually heated to 180°C. Secondly, 143.33 g 1,4-dichlorobenzene (0.975 mol) and 5.88 g 2,5-dichloroterephthalic acid (0.025 mol) were added when the reactor was cooled down to 130°C. Then, the reaction temperature was raised to 200°C and maintained for 2 h. Finally, the temperature of the reaction was slowly raised to 240°C for 6 h, and after the reaction was over, the temperature was cooled by condensate water. The above reaction is carried out at 3-10 atmospheric pressure. The product was cleaned with hydrochloric acid and hot deionized water and dried at 100°C for 24 h to obtain PPS-2COOH (2.5).

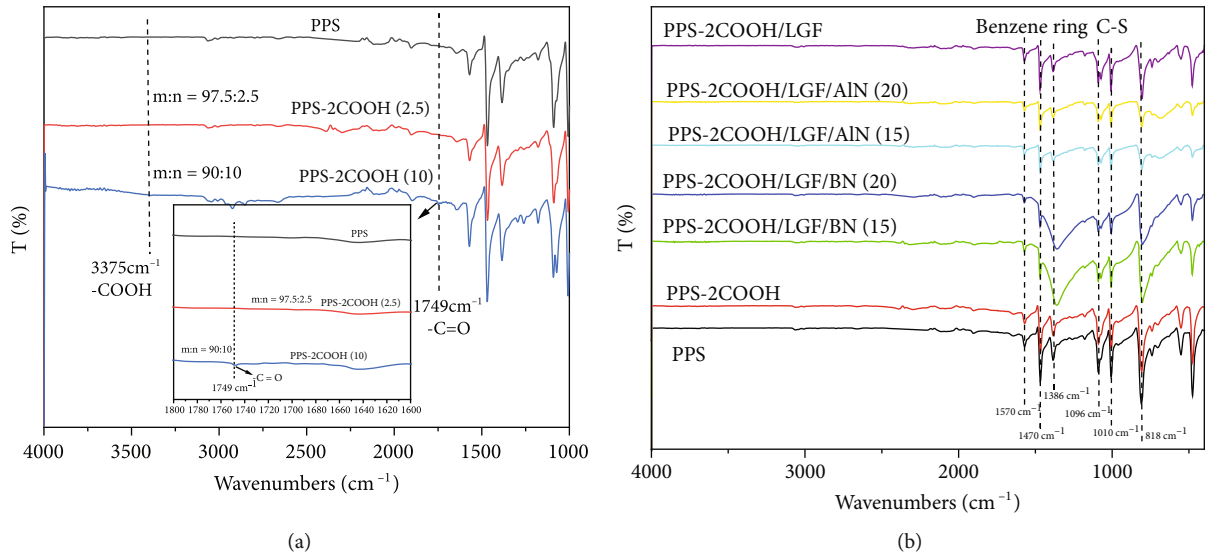

(a) (b)

Figure 1: (a) FT-IR spectra of PPS and copolymer PPS-COOH at 4000-1000 cm^{-1}; (b) FT-IR spectra of PPS, PPS-2COOH, PPS-2COOH/LGF/BN, and PPS-2COOH/LGF/AlN at 4000-400 cm^{-1}.

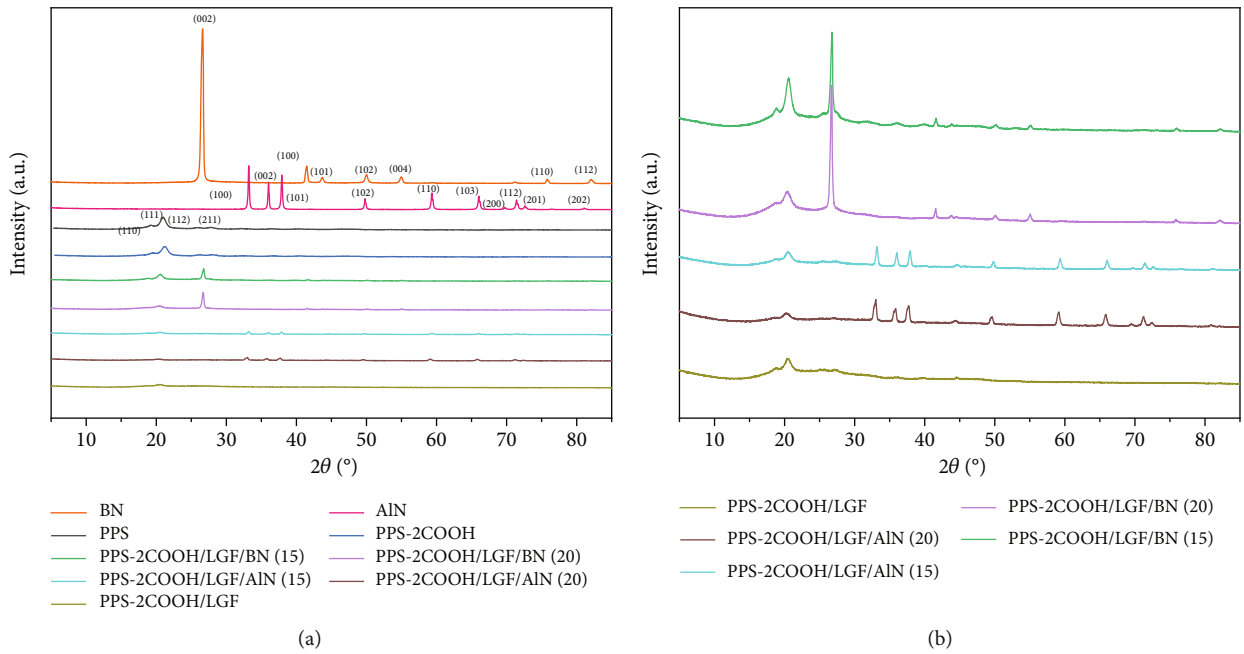

(a) (b)

Figure 2: (a) XRD patterns of PPS, PPS-2COOH, BN, AlN, PPS-2COOH/LGF/BN and PPS-2COOH/LGF/AlN; (b) XRD images of the composites.

2.3. Preparation of Composites. The composites of BN, AlN, and PPS-2COOH were prepared by melt mixing. And the composites were prepared according to the following procedures: (i) all raw materials were dried for 24 h in a vacuum oven before processing. (ii) In a high-speed pulverizer (Beijing Ever Bright Medical Treatment Instrument Co., Ltd.), the filler and glass fiber were mixed with PPS-COOH powder. The homogenized mixture was melted and mixed at 310°C in a micro extruder (HAAK miniLab II). The compositions of the obtained composites are shown in Table 1.

3. Characterization

FT-IR analysis was performed using 170SX (Thermo Nicolet Corporation, USA) with a spectral wavenumber set to 400-4000 cm^{-1}.

The X-ray diffraction pattern was tested by X-ray diffractometer (XRD; PANalytical B.V., X Pert Pro MPD DY129, Netherlands). The diffraction angle was set as 10°-80°, copper was used as the target, the working voltage was 40 kV, the working current was 25 mA, and the scanning rate was 2°/min.

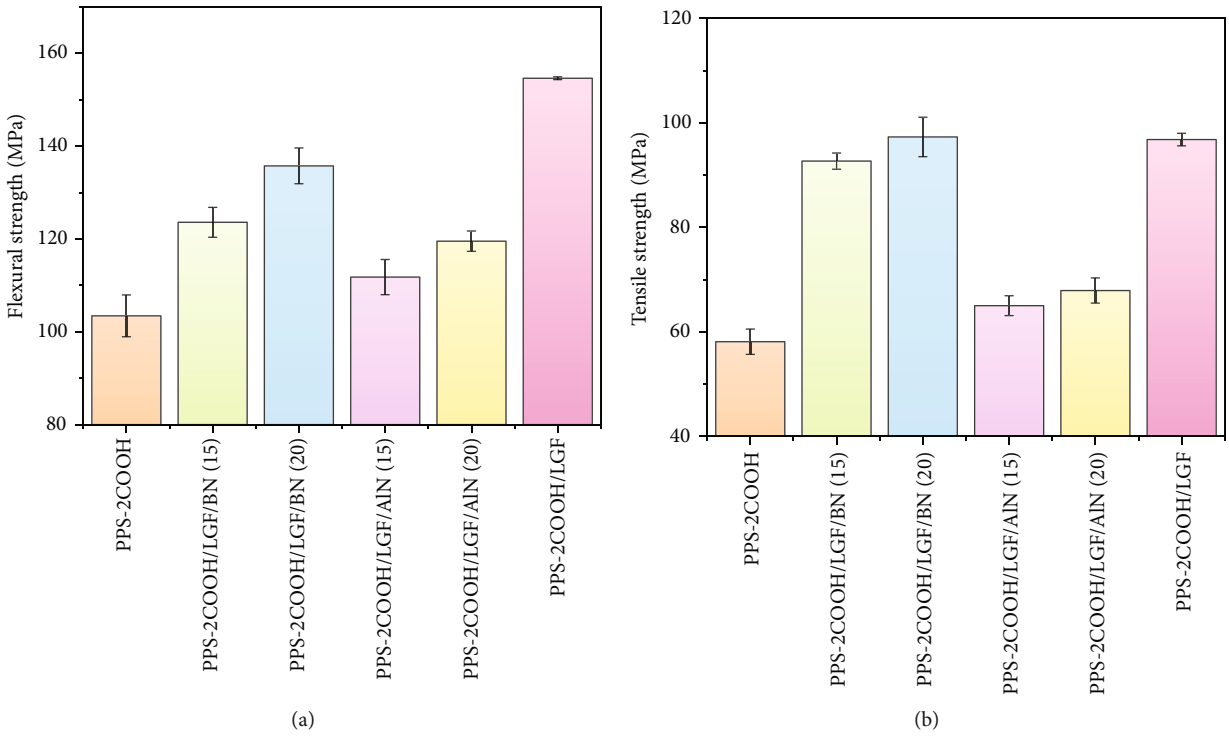

Figure 3: (a) Flexural strength and (b) tensile strength of PPS-2COOH, PPS-2COOH/LGF/BN, and PPS-2COOH/LGF/AlN.

The flexural strength and tensile strength of the samples were examined using the MTS E45.105 electronic universal testing machine (MTS Corporation, America) at a rate of 5 mm/min and 2 mm/min, respectively.

The morphologies of the composites were observed by scanning electron microscope (SEM; FEI Corporation, Nova Nano SEM 450, American)/energy dispersive spectrometry (EDS; Oxford Instruments, OXFORD Ultim Extreme EDS, America,). Before observation, the samples were subjected to a sputtering procedure that coated them in a layer of gold and palladium.

Differential scanning calorimetry (DSC) analysis of samples was performed using the DSC3+/500 thermal analyzer (Mettler-Toledo Corporation, Switzerland) at 10°C/min (nitrogen atmosphere) over the entire temperature range (25-300°C), rising from room temperature to 300°C and then down to room temperature. The thermogravimetric analysis was performed using TGA Q500 V6.4 Build 193, and the test temperature range was from 30°C to 800°C, with a temperature change rate of 10°C/min.

According to the standard GB/T 22588-2008, the LFA467 laser thermal conductivity instrument (LFA; Netzsch Instruments Co., Nanoflash LFA 467 system, Germany) measured the thermal diffusivity of a sample. Using the following formula to calculate the thermal conductivity of the composite at room temperature [45]:

$$\lambda = \alpha \times \rho \times C_p, \tag{1}$$

where λ, α, ρ, and C_p represent the thermal conductivity (W/mK), thermal diffusivity (m^2/s), density (kg/m^3), and specific heat capacity (J/(kg·K)), respectively. The C_p of the composites was measured by differential scanning calorimetry (DSC), using the sapphire method. The DSC curve of a standard sapphire (with known specific heat capacity) was tested under a nitrogen atmosphere with a temperature rise rate of 10°C/min and a temperature setting range of 0-100°C. The DSC curve was then converted to the specific heat capacity of the sample to be measured by the formula:

$$C_p = C_1 \cdot \frac{(Y_2 - Y_0) \cdot m_1}{(Y_1 - Y_0) \cdot m_2}, \tag{2}$$

where m_1, m_2, Y_0, Y_1, Y_2, C_1, and C_p represent the mass of the sapphire (mg), the mass of the sample (mg), the DSC value of baseline, the DSC value of the sapphire, the DSC value of the sample to be tested, the specific heat capacity of the sapphire (J/(mg·K)), and the specific heat capacity of sample to be tested (J/(mg·K)), respectively.

The dielectric constant and dielectric loss of the samples were measured using Broadband Dielectric Spectrometer CONCEPT 50 (Novocontrol Corporation, Germany) at room temperature.

The solubility of 0.2 g samples that was immersed in 25 mL of different solvent was examined at room temperature, the results were recorded in detail.

4. Results and Discussion

4.1. Infrared Analysis. Figure 1 shows the FT-IR spectrum of PPS, PPS-2COOH, and composites. From Figure 1(a), PPS and PPS-2COOH had almost the same characteristic absorption, which may be due to the low content of the carboxyl group and the inconspicuous characteristic peak. After

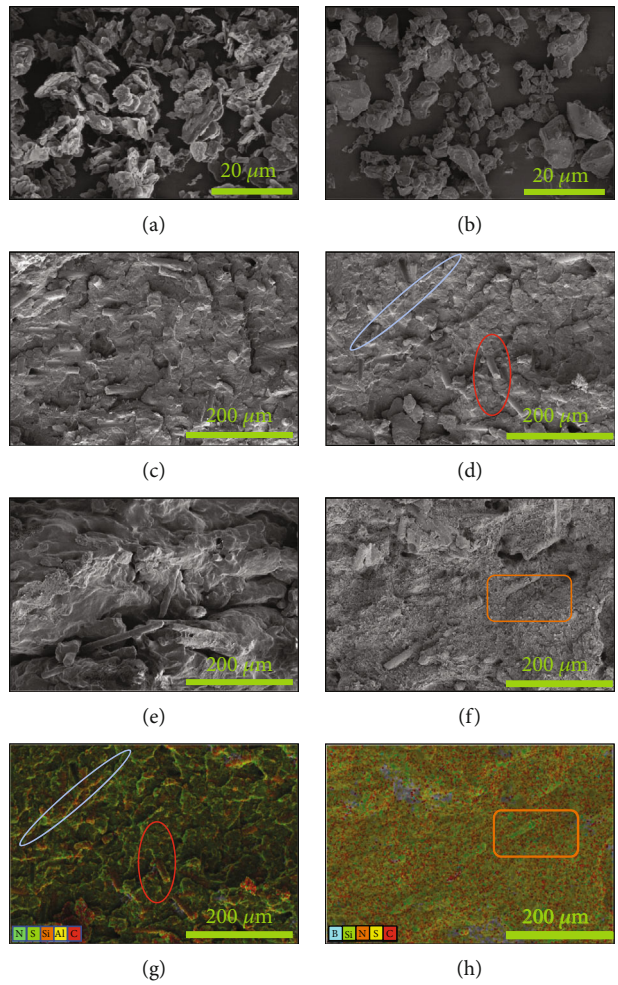

Figure 4: FE-SEM cross-sectional images of PPS-2COOH/LGF/AlN and PPS-2COOH/LGF/BN composite films: (a) BN (20 μm); (b) AlN (20 μm); (c) PPS-2COOH/LGF/AlN (15) (200 μm); (d) PPS-2COOH/LGF/AlN (20) (200 μm); (e) PPS-2COOH/LGF/BN (15) (200 μm); (f) PPS-2COOH/LGF/BN (20) (200 μm); (g) EDS mapping of (d) (200 μm); (h) EDS mapping of (f) (200 μm).

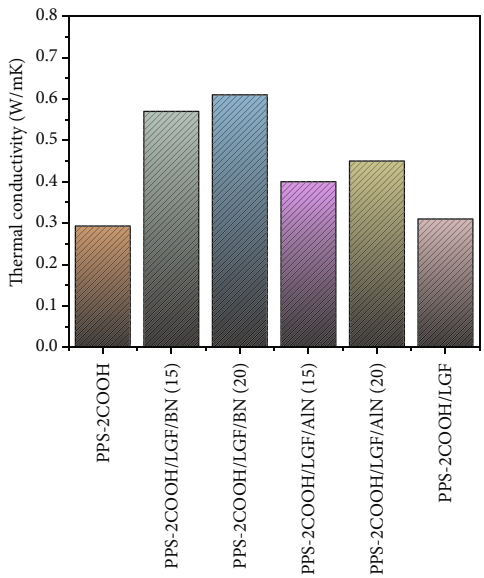

Figure 5: Effect of different fillers on λ of PPS-2COOH, PPS-2COOH/LGF/BN, and PPS-2COOH/LGF/AlN.

increasing the carboxyl content, the unsharp peak at 3375 cm^{-1} could be attributed to the stretching vibration of -COOH, and the new peaks at about 1749 cm^{-1} of the copolymer was attributed to the stretching vibration of -C=O, which can prove that the synthesis method is successful. In the infrared spectrum of PPS, the peak near 1570 cm^{-1} was the symmetric stretching vibration peak of the benzene ring [46]. The stretching vibration peak of the C=C bond in the benzene ring was around 1470 cm^{-1}. The hydrogen atoms in the parasubstituted benzene ring vibrated primarily in two directions: in-plane bending vibration peaked at around 1010 cm^{-1}, whereas out-of-plane deformation vibration peaked at about 818 cm^{-1}. Saëki [47, 48] made a detailed analysis of the infrared spectrum of 1,4-dichlorobenzene. Compared with the FT-IR results of 1,4-dichlorobenzene, the absorption peak of the thioether bond appeared in the FT-IR of PPS and its copolymer, indicating that PPS and its copolymer were successfully synthesized in this work. 1096 cm^{-1} is the absorption peak of the C-S bond [40]. The infrared spectrogram of PPS-2COOH could not be distinguished from PPS due to the low content of the carboxyl

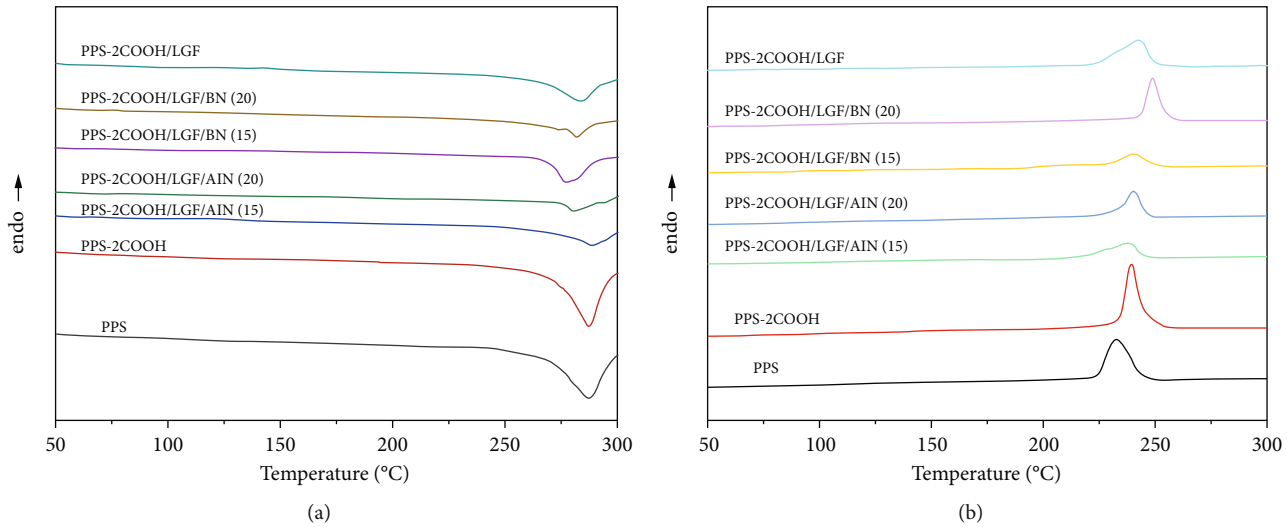

Figure 6: DSC curves of PPS, PPS-2COOH, PPS-2COOH/LGF/BN, and PPS-2COOH/LGF/AlN in a nitrogen atmosphere.

Table 2: Thermal properties of the PPS-2COOH/LGF/AlN and PPS-2COOH/LGF/BN composites.

Samples	T_m (°C)	T_c (°C)	$T_{5\%}$ (°C)
PPS-2COOH/LGF/BN (15)	281.3	242.2	580.5
PPS-2COOH/LGF/BN (20)	281.5	248.4	506.3
PPS-2COOH/LGF/AlN (15)	288.0	236.4	510.4
PPS-2COOH/LGF/AlN (20)	280.8	248.4	511.6
PPS-2COOH/LGF	283.3	242.1	509.6
PPS-2COOH	287.1	239.0	495.7
PPS	286.7	231.6	499.8

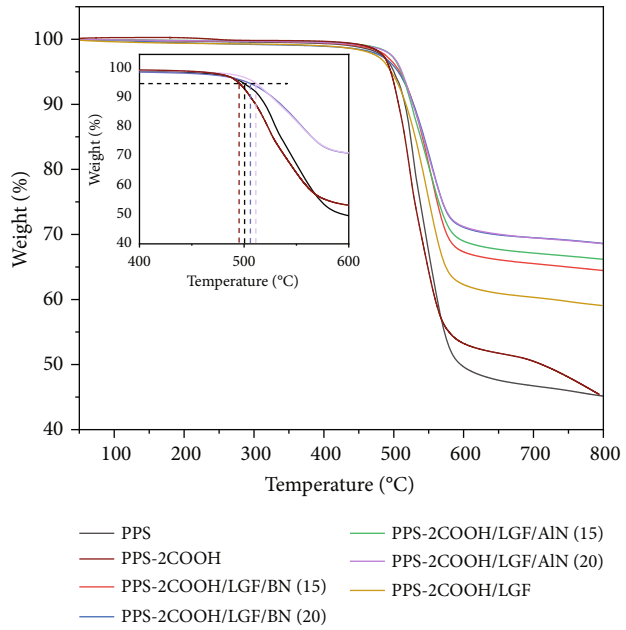

Figure 7: TGA curves of PPS, PPS-2COOH, PPS-2COOH/LGF/BN, and PPS-2COOH/LGF/AlN in a nitrogen atmosphere.

group, indicating that they had comparable structural characteristics.

4.2. Crystal Structure Analysis. Figure 2 displays the XRD patterns of the composite materials, ceramic filler, polymer PPS, and PPS-2COOH. The principle reflection of BN is located near 2θ~26.67° and can be classified as (002) reflection of graphitic structure. At the same time, other much weaker peaks corresponding to the (100)/(101) reflection were observed near about 42.30° [49]. The peak of AlN conforms to JCPDS NO.76-0565, and there is no other phase in the spectrum, indicating that the sample phase is pure [50]. With the increase of BN/AlN content, the characteristic peak of BN/AlN in composites becomes more obvious. The 2θ value of pure PPS was 19.21°, 20.87°, 25.97°, and 27.87°, corresponding to (110), (111), (112), and (211) crystal planes, respectively [51]. From Figure 2, the diffraction peak position of PPS-2COOH was not significantly different from that of PPS, indicating that the crystal shape of the PPS-2COOH polymer chain is consistent with PPS after the introduction of carboxylic acid side groups. The addition of inorganic fillers did not change the crystal structure of PPS-2COOH.

4.3. Mechanical Property. Generally, glass fiber can be used as mechanical reinforcement, and BN/AlN can improve the thermal and mechanical properties of composites. The mechanical properties of PPS-2COOH and its composites are shown in Figure 3. The tensile strength and flexural strength of PPS-2COOH/LGF had increased compared to PPS-2COOH, which was due to the addition of fiber into the composite material. On the one hand, the fiber was responsible for carrying the majority of the load when the composite underwent stress because it was able to transmit local loads over long distances by way of its ability to transfer loads across interfaces [52]. On the other hand, a strong interaction between the carboxyl group from the matrix and the silicon hydroxyl from LGF might be formed, according to previous reports [40, 41, 53]. Compared with PPS-2COOH/LGF/BN and PPS-2COOH/LGF/AlN, PPS-

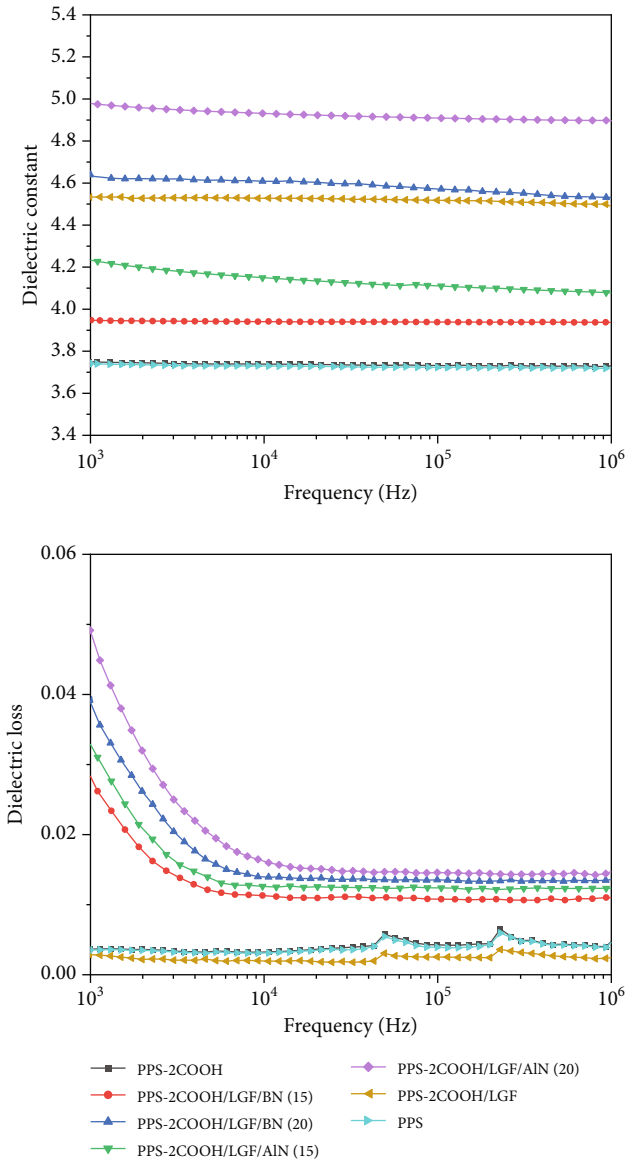

Figure 8: Effect of ceramic filler content on the ε and tan δ value of composites at a different frequency.

2COOH/LGF showed optimal mechanical strength, which proved that the improvement of mechanical properties of composites was mainly due to the addition of LGF. In this work, BN (similar to graphite layered structure) has a much higher surface area. In return, resulting much higher polymer-filler interaction compared to AlN particles [54, 55]. At the same time, the particle size, content, and distribution of inorganic fillers will also affect the mechanical properties of the composites [56]. This series of comprehensive factors may lead to a better matrix-BN reinforcement effect. In general, all composites had good mechanical properties.

4.4. Morphology of Fracture Surfaces. To investigate the dispersion of all fillers in the PPS matrix, PPS-2COOH/LGF/BN and PPS-2COOH/LGF/AlN were studied by SEM, respectively. The SEM photos are shown in figure 4. AlN had an irregular granular form (Figure 4(b)), and the shape of BN was a sheet with a smooth surface (Figure 4(a)). The AlN content of composites in Figures 4(c) and 4(d) was 15 wt% and 20 wt%, respectively. As can be observed, the dispersion was quite uniform and the surface was rough, suggesting that the combination worked well. The bright spot in Figure 4(d) may be the AlN particle, which was consistent with the EDS image (Figure 4(g)). As indicated by the green border, the brighter part of Figure 4(d) coincided with the yellow part of Figure 4(g). Figures 4(e) and 4(f) were SEM images of composite materials which contained 15 wt% and 20 wt% BN, respectively. Both Figure 4(e) and Figure 4(f) had holes, and the rod-like glass fibers could be seen clearly from the EDS mapping, the fibers were adhered tightly by the matrix. Figure 4(g) was a mapping diagram of composite PPS-2COOH/LGF/AlN (20), and the results also showed that fibers and particles had good dispersion properties in the matrix.

4.5. Thermal Conductivities of Composites. Figure 5 shows the thermal conductivity (λ(W/mK)) of composites with different mass fractions of BN and AlN added. When only 25 wt% LGF was added, there was no significant difference in the λ(W/mK) value between the composites PPS-2COOH/LGF and PPS-2COOH matrix. Under the same packing load, the λ(W/mK) value of the PPS-2COOH/LGF/BN(AlN) composite was higher than that of the PPS-2COOH/LGF composite, indicating that the thermal conductivity of composites mainly depends on the ceramic filler, and the ceramic fillers BN and AlN were proved to have excellent thermal conductivity [28, 57]. The values of the thermal conductivity of PPS-2COOH/LGF/BN and PPS-2COOH/LGF/AlN composites significantly increased with an increase in ceramic filler content. This was primarily because an increase in ceramic filler increased the likelihood of effective contact and overlap between fillers and made it simpler to form a continuous thermal conductivity network and path in the system, improving the thermal conductivity of the PPS-2COOH composite.

4.6. Thermal Properties. The thermal behavior of PPS, PPS-2COOH, and composites was examined by DSC, as shown in Figure 6 and Table 2. The melting point (T_m) of PPS-COOH (287.1°C) was higher than that of pure PPS (286.7°C), mainly because the introduction of carboxyl group enhanced the interaction between copolymer molecular chains, and its influence on the increase of melting point of copolymer might be higher than that of carboxyl group which would destroy the law of molecular chains, resulting in the increase of melting point of the copolymer. As shown in Figure 6(b), the crystallization temperature (T_c) of the composites were all higher than that of PPS-2COOH, indicating that the crystallization process of PPS-2COOH resin is directly affected by the inorganic filler acting as heterogeneous nucleating agent.

The TGA curves of PPS, PPS-2COOH, and composites are shown in Figure 7. PPS exhibited strong thermal stability and its loss temperature of 5 wt% ($T_{5\%}$) was approximately 499.8°C, while the $T_{5\%}$ of PPS-2COOH was about 495.7°C.

Table 3: Solubility of PPS-2COOH and its composites.

Samples solvent	2.5% PPS-2COOH	PPS-2COOH/LGF/AlN (15)	PPS-2COOH/LGF/AlN (20)	PPS-2COOH/LGF/BN (15)	PPS-2COOH/LGF/BN (20)	PPS-2COOH/LGF/
DMF	—	—	—	—	—	—
Ethanol	—	—	—	—	—	—
DMAC	—	—	—	—	—	—
HCL	—	—	—	—	—	—
NMP	—	—	—	—	—	—
Dichloromethane	—	—	—	—	—	—
1 mol/L NaOH	—	—	—	—	—	—
Tetrahydrofuran	—	—	—	—	—	—
Acetonitrile	—	—	—	—	—	—
Dichloroethane	—	—	—	—	—	—
Xylene	—	—	—	—	—	—
Aqua regia	—	—	—	—	—	—

-: insoluble.

This difference was mostly caused by the addition of the carboxyl group, which caused the polymer decarboxylation reaction to take place at a lower temperature. The thermal decomposition temperature of the composites with AlN and BN was significantly increased, and the $T_{5\%}$ of PPS-2COOH/LGF/AlN (20) and PPS-2COOH/LGF/BN (20) reached up to 511.6°C and 506.3°C, respectively. This indicates that there is a certain molecular force between the polymer molecular chain and the inorganic filler, which makes it difficult to move, thus increasing the decomposition temperature of the composite material. PPS-2COOH was less likely to decompose at high temperatures because AlN and BN have larger heat capacities and thermal conductivities than the PPS-2COOH chain, which can absorb heat well. This outcome demonstrated that the filled PPS-2COOH can be used as a thermal material in high-temperature applications.

4.7. Dielectric Properties of Composites. Figure 8 shows the dielectric constant (ε) and dielectric loss values (tan δ) of composites with different mass fractions of BN and AlN added at different test frequencies. After the introduction of carboxyl groups, the dielectric constant of PPS increased slightly, because the ε value of the polymer is determined by the performance and arrangement of bonds in the backbone structure, and the more polar substituents, the greater the dielectric constant and dielectric loss. As the filler content increased, the composite ε and tan δ values both increase slightly. Due to the comparatively high dielectric constant of aluminum nitride and the improved polarization property of composites caused by the dipole interaction between nearby particles, the parameters of composites with AlN were greater than that of BN. The ε and tan δ of composites decreased with increasing frequency, possibly because dipoles in polymer samples tend to be oriented in the direction of the applied electric field. However, after increasing to a certain frequency, the dielectric characteristics hardly change with the frequency increase, which may be related to the direction of the dipole, which makes it difficult to rotate at high frequencies [58]. Overall, the results showed that the composite material containing BN had a low dielectric constant and could be used as a low-dielectric material.

4.8. Solubility Analysis. As shown in Table 3, the solubility of PPS-2COOH and its composites in different solvents was tested. Table 3 shows that PPS-2COOH and its composites are insoluble in any solvent at room temperature, which proves the excellent solvent resistance of the composites.

5. Conclusions

In this study, PPS-2COOH containing carboxyl groups was successfully prepared and applied to the preparation of two composite materials. PPS-2COOH had a similar chemical structure to PPS and maintained its excellent chemical resistance. In composites, the filler BN and AlN filler were evenly dispersed in the matrix. With the increases in BN/AlN content, the thermal conductivity of the composites increased due to a continuous thermal conductivity network and path in the system. In addition, all the composites PPS-2COOH/LGF/BN(AlN) showed low dielectric constants and dielectric losses, indicating they had application prospects in terms of high thermal conductivity and low dielectric.

Data Availability

Data is openly available in a public repository.

Conflicts of Interest

The authors declare that they have no conflicts of interest.

Acknowledgments

This work was financially supported by the Science Specialty Program of Sichuan University(Grand No. 2020SCUNL210).

References

[1] M. M. Silva and J. Guerreiro, "On the 5G and beyond," *Applied Sciences*, vol. 10, no. 20, p. 7091, 2020.

[2] R. K. Goyal, A. N. Tiwari, U. P. Mulik, and Y. S. Negi, "Effect of aluminum nitride on thermomechanical properties of high performance PEEK," *Composites Part A: Applied Science and Manufacturing*, vol. 38, no. 2, pp. 516–524, 2007.

[3] X. Huang, B. Sun, Y. Zhu, S. Li, and P. Jiang, "High- _k_ polymer nanocomposites with 1D filler for dielectric and energy storage applications," *Progress in Materials Science*, vol. 100, pp. 187–225, 2019.

[4] M. D. Hill, D. B. Cruickshank, and I. A. MacFarlane, "Perspective on ceramic materials for 5G wireless communication systems," *Applied Physics Letters*, vol. 118, no. 12, article 120501, 2021.

[5] G.-W. Lee, M. Park, J. Kim, J. I. Lee, and H. G. Yoon, "Enhanced thermal conductivity of polymer composites filled with hybrid filler," *Composites Part A: Applied Science and Manufacturing*, vol. 37, no. 5, pp. 727–734, 2006.

[6] P. Zuo, A. Tcharkhtchi, M. Shirinbayan, J. Fitoussi, and F. Bakir, "Overall investigation of poly (phenylene sulfide) from synthesis and process to applications—a review," *Macromolecular Materials and Engineering*, vol. 304, no. 5, p. 1800686, 2019.

[7] H. Li, G. Y. Lv, G. Zhang, H. H. Ren, X. X. Fan, and Y. G. Yan, "Synthesis and characterization of novel poly(phenylene sulfide) containing a chromophore in the main chain," *Polymer International*, vol. 63, no. 9, pp. 1707–1714, 2014.

[8] M. A. Maaroufi, Y. Carpier, B. Vieille, L. Gilles, A. Coppalle, and F. Barbe, "Post-fire compressive behaviour of carbon fibers woven-ply Polyphenylene sulfide laminates for aeronautical applications," *Composites Part B: Engineering*, vol. 119, pp. 101–113, 2017.

[9] B. L. Zhu, J. Ma, J. Wu, K. C. Yung, and C. S. Xie, "Study on the properties of the epoxy-matrix composites filled with thermally conductive AlN and BN ceramic particles," *Journal of Applied Polymer Science*, vol. 118, no. 5, pp. 2754–2764, 2010.

[10] B. L. Zhu, H. Zheng, J. Wang, J. Ma, J. Wu, and R. Wu, "Tailoring of thermal and dielectric properties of LDPE-matrix composites by the volume fraction, density, and surface modification of hollow glass microsphere filler," *Composites Part B: Engineering*, vol. 58, pp. 91–102, 2014.

[11] B. L. Zhu, J. Wang, H. Zheng et al., "Thermal conductivity and dielectric properties of immiscible LDPE/epoxy blend filled with hybrid filler consisting of HGM and nitride particle," *Journal of Alloys and Compounds*, vol. 701, pp. 499–507, 2017.

[12] B. L. Zhu, J. Wang, H. Zheng, J. Ma, J. Wu, and R. Wu, "Investigation of thermal conductivity and dielectric properties of LDPE-matrix composites filled with hybrid filler of hollow glass microspheres and nitride particles," *Composites Part B: Engineering*, vol. 69, pp. 496–506, 2015.

[13] Z. C. Lule and J. Kim, "Organic-inorganic hybrid filler for improved thermal conductivity and anti- dripping performance of polybutylene succinate composite," *Journal of Cleaner Production*, vol. 340, article 130781, 2022.

[14] Y. Chai, X. Zhou, H. Zhang, and Y. Zhang, "The effect of heat treatment on the properties of SiCf/SiC composites prepared with different SiC fibers," *Fusion Science and Technology*, vol. 75, no. 2, pp. 112–119, 2019.

[15] S. Choi and J. Kim, "Thermal conductivity of epoxy composites with a binary-particle system of aluminum oxide and aluminum nitride fillers," *Composites Part B: Engineering*, vol. 51, pp. 140–147, 2013.

[16] N. N. T. Nam and M. Koshino, "Erratum: Lattice relaxation and energy band modulation in twisted bilayer graphene [Phys. Rev. B96, 075311 (2017)]," *Physical Review B*, vol. 101, no. 9, p. 5, 2020.

[17] X. Huang, W. Liu, S. Li, P. Jiang, and T. Tanaka, "Boron nitride based poly (phenylene sulfide) composites with enhanced thermal conductivity and breakdown strength," *IEEJ Transactions on Fundamentals and Materials*, vol. 133, no. 3, pp. 66–70, 2013.

[18] S. Ryu, K. Kim, and J. Kim, "Silane surface modification of boron nitride for high thermal conductivity with polyphenylene sulfide via melt mixing method," *Polymers for Advanced Technologies*, vol. 28, no. 11, pp. 1489–1494, 2017.

[19] M. N. Ge, Q. Q. Li, J. F. Zhang et al., "Enhancing thermal conductivity of the insulating layer of high-frequency copper clad laminates via incorporating surface modified spherical hBN fillers," *Journal of Materials Science: Materials in Electronics*, vol. 31, no. 5, pp. 4214–4223, 2020.

[20] S. Akkoyun and M. Akkoyun, "Improvement of thermal conductivity of rigid polyurethane foams with aluminum nitride filler," *Cellular Polymers*, vol. 40, no. 2, pp. 87–98, 2021.

[21] S. Dai, T. Zhang, S. Mo et al., "Study on preparation, thermal conductivity, and electrical insulation properties of epoxy/AlN," *IEEE Transactions on Applied Superconductivity*, vol. 29, no. 2, pp. 1–6, 2019.

[22] S. Yu, W. M. Wong, X. Hu, and Y. K. Juay, "The characteristics of carbon nanotube-reinforced poly(phenylene sulfide) nanocomposites," *Journal of Applied Polymer Science*, vol. 113, no. 6, pp. 3477–3483, 2009.

[23] G. Pircheraghi, T. Powell, V. Solouki Bonab, and I. Manas-Zloczower, "Effect of carbon nanotube dispersion and network formation on thermal conductivity of thermoplastic polyurethane/carbon nanotube nanocomposites," *Polymer Engineering & Science*, vol. 56, no. 4, pp. 394–407, 2016.

[24] K. H. Jung, H. J. Kim, M. H. Kim, and J.-C. Lee, "Preparation of poly (phenylene sulfide)/nylon 6 grafted graphene oxide nanocomposites with enhanced mechanical and thermal properties," *Macromolecular Research*, vol. 28, no. 3, pp. 241–248, 2020.

[25] D. Han, P. Xie, G. Fan et al., "Three-dimensional graphene network supported by poly phenylene sulfide with negative permittivity at radio-frequency," *Journal of Materials Science: Materials in Electronics*, vol. 29, no. 24, pp. 20768–20774, 2018.

[26] M. Choi, J. Kim, Y. Oh et al., "Surface modification of sulfur-assisted reduced graphene oxide with poly (phenylene sulfide) for multifunctional nanocomposites," *Polymers*, vol. 14, no. 4, p. 732, 2022.

[27] Y. Guo, K. Ruan, X. Shi, X. Yang, and J. Gu, "Factors affecting thermal conductivities of the polymers and polymer composites: a review," *Composites Science and Technology*, vol. 193, article 108134, 2020.

[28] B. Guo, Q. Lin, X. Zhao, and X. Zhou, "Crystallization of polyphenylene sulfide reinforced with aluminum nitride composite: effects on thermal and mechanical properties of the composite," *Iranian Polymer Journal*, vol. 24, no. 11, pp. 965–975, 2015.

[29] H. Zhai, X. Zhou, L. Fang, and A. Lu, "Study on mechanical properties of powder impregnated glass fiber reinforced poly(-phenylene sulphide) by injection molding at various temperatures," *Journal of Applied Polymer Science*, vol. 115, no. 4, pp. 2019–2027, 2010.

[30] S. F. Zhou, Q. X. Zhang, C. Q. Wu, and J. Huang, "Effect of carbon fiber reinforcement on the mechanical and tribological properties of polyamide6/polyphenylene sulfide composites," *Materials & Design*, vol. 44, pp. 493–499, 2013.

[31] A. P. Costa, E. C. Botelho, and L. C. Pardini, "Influence of environmental conditioning on the shear behavior of poly(phenylene sulfide)/glass fiber composites," *Journal of Applied Polymer Science*, vol. 118, no. 1, pp. 180–187, 2010.

[32] M. Jiang, X. Zou, Y. Huang, and X. Liu, "The effect of bismaleimide on thermal, mechanical, and dielectric properties of allyl-functional bisphthalonitrile/bismaleimide system," *High Performance Polymers*, vol. 29, no. 9, pp. 1016–1026, 2017.

[33] D. Ren, K. Li, L. Chen et al., "Modification on glass fiber surface and their improved properties of fiber- reinforced composites via enhanced interfacial properties," *Composites Part B: Engineering*, vol. 177, article 107419, 2019.

[34] A. V. Longobardo, "Glass fibers for printed circuit boards," in *Fiberglass and Glass Technology*, F. Wallenberger and P. Bingham, Eds., Springer, Boston, MA, 2010.

[35] Z. Zhang, L. Yuan, G. Liang, and A. Gu, "Fabrication and origin of flame retarding glass fiber/bismaleimide resin composites with high thermal stability, good mechanical properties, and a low dielectric constant and loss for high frequency copper clad laminates," *RSC Advances*, vol. 6, no. 24, pp. 19638–19646, 2016.

[36] J. Guo, H. Wang, C. Zhang, Q. Zhang, and H. Yang, "MPPE/SEBS composites with low dielectric loss for high-frequency copper clad laminates applications," *Polymers*, vol. 12, no. 9, p. 1875, 2020.

[37] M. Zhang, X. Wang, Y. Bai, Z. Li, and B. Cheng, "C_{60} as fine fillers to improve poly(phenylene sulfide) electrical conductivity and mechanical property," *Scientific Reports*, vol. 7, no. 1, p. 4443, 2017.

[38] X. Li, D. Xu, N. Gong, Z. Xu, L. Wang, and W. Dong, "Improving the strength of injection molded aluminum/polyphenylene sulfide lap joints dependence on surface microstructure and composition," *Materials & Design*, vol. 179, article 107875, 2019.

[39] K. Kim, J. Lee, S. Ryu, and J. Kim, "Laser direct structuring and electroless plating applicable super-engineering plastic PPS based thermal conductive composite with particle surface modification," *RSC Advances*, vol. 8, no. 18, pp. 9933–9940, 2018.

[40] Y. Dong, T. Yu, X.-j. Wang et al., "Improved interfacial shear strength in polyphenylene sulfide/carbon fiber composites via the carboxylic polyphenylene sulfide sizing agent," *Composites Science and Technology*, vol. 190, article 108056, 2020.

[41] H.-h. Ren, D.-x. Xu, G.-m. Yan et al., "Effect of carboxylic polyphenylene sulfide on the micromechanical properties of polyphenylene sulfide/carbon fiber composites," *Composites Science and Technology*, vol. 146, pp. 65–72, 2017.

[42] K. Zhang, G. Zhang, B. Liu, X. Wang, S. Long, and J. Yang, "Effect of aminated polyphenylene sulfide on the mechanical properties of short carbon fiber reinforced polyphenylene sulfide composites," *Composites Science and Technology*, vol. 98, pp. 57–63, 2014.

[43] F. Huang, Y. Yuan, Z. Jiang, B. Tang, and S. Zhang, "Microstructures and properties of glass fiber reinforced PTFE composite substrates with laminated construction," *Materials Research Express*, vol. 6, no. 7, article 075305, 2019.

[44] W. Li, H. Yin, Z. Chen et al., "inventors; Preparation method for polyphenylene sulfide and polyphenylene sulfide prepared by means of same," patent EP3677617.

[45] M. Kim, J. Lee, M. Cho, and J. Kim, "Improvement of thermal and abrasion resistance performance of polyphenylene sulfide composite through 3-mercaptopropyl trimethoxysilane treatment of carbon fiber and graphene oxide fillers," *Polymer Testing*, vol. 108, article 107517, 2022.

[46] Y. Shi, Y. Bai, Y. Lei et al., "Simultaneously enhanced heat dissipation and tribological properties of polyphenylene sulfide-based composites via constructing segregated network structure," *Journal of Materials Science and Technology*, vol. 99, pp. 239–250, 2022.

[47] S. Saëki, "Raman Spectra ofp-Dichlorobenzene andp-Dichlorobenzene-d4," *Bulletin of the Chemical Society of Japan*, vol. 34, no. 11, pp. 1658–1664, 1961.

[48] S. Saëki, "The infrared absorption spectra ofp-Dichlorobenzene andp-Dichlorobenzene-d4," *Bulletin of the Chemical Society of Japan*, vol. 35, no. 2, pp. 326–332, 1962.

[49] B. Matović, J. Luković, M. Nikolić et al., "Synthesis and characterization of nanocrystaline hexagonal boron nitride powders: XRD and luminescence properties," *Ceramics International*, vol. 42, no. 15, pp. 16655–16658, 2016.

[50] C.-Y. Zhang, Y.-L. Yu, H. Yang et al., "Mechanism for the hydrolysis resistance of aluminum nitride powder modified by boric acid," *Ceramics International*, vol. 48, no. 22, pp. 32696–32702, 2022.

[51] C. F. Brucker, "Electron spectroscopy: Theory, techniques and applications, vol. 4. C. R. Brundle and A. D. Baker (Editors). Academic Press London, 1982," *Surface and Interface Analysis*, vol. 4, no. 6, pp. i–ii, 1982.

[52] L. Zhao, Y. Yu, H. Huang et al., "High-performance polyphenylene sulfide composites with ultra-high content of glass fiber fabrics," *Composites Part B: Engineering*, vol. 174, article 106790, 2019.

[53] H.-H. Ren, D.-X. Xu, T. Yu et al., "Effect of polyphenylene sulfide containing amino unit on thermal and mechanical properties of polyphenylene sulfide/glass fiber composites," *Journal of Applied Polymer Science*, vol. 135, no. 6, article 45804, 2018.

[54] M. B. Alanalp, A. Durmus, and I. Aydin, "Quantifying effect of inorganic filler geometry on the structural, rheological and viscoelastic properties of polypropylene-based thermoplastic elastomers," *Journal of Polymer Research*, vol. 26, no. 2, p. 46, 2019.

[55] T. Natsuki and J. Natsuki, "Prediction of mechanical properties for hexagonal boron nitride nanosheets using molecular mechanics model," *Applied Physics A*, vol. 123, no. 4, p. 283, 2017.

[56] P. Sahoo, A. Chaturvedi, U. Ramamurty, and H. Matte, "Nanomechanical study of aqueous-processed h-BN reinforced PVA composites," *Nanotechnology*, vol. 34, no. 9, article 095703, 2023.

[57] J. Gu, Y. Guo, X. Yang et al., "Synergistic improvement of thermal conductivities of polyphenylene sulfide composites filled with boron nitride hybrid fillers," *Composites Part A: Applied Science and Manufacturing*, vol. 95, pp. 267–273, 2017.

[58] A. M. Díez-Pascual and A. L. Díez-Vicente, "High-performance aminated poly (phenylene sulfide)/ZnO nanocomposites for medical applications," *ACS Applied Materials & Interfaces*, vol. 6, no. 13, pp. 10132–10145, 2014.